International Journal of Nanomedicine

Dovepress
open access to scientific and medical research

Open Access Full Text Article

ORIGINAL RESEARCH

Platelet Membrane-Coated Nanoparticles Target Sclerotic Aortic Valves in ApoE$^{-/-}$ Mice by Multiple Binding Mechanisms Under Pathological Shear Stress

This article was published in the following Dove Press journal:
International Journal of Nanomedicine

Hongbo Yang[1,*]
Yanan Song[1,*]
Jing Chen[1,*]
Zhiqing Pang[2]
Ning Zhang[1]
Jiatian Cao[1]
Qiaozi Wang[1]
Qiyu Li[1]
Feng Zhang[1]
Yuxiang Dai[1]
Chenguang Li[1]
Zheyong Huang[1]
Juying Qian[1]
Junbo Ge[1]

[1]Department of Cardiology, Zhongshan Hospital, Fudan University, Shanghai Institute of Cardiovascular Diseases, Shanghai 200032, People's Republic of China; [2]School of Pharmacy, Key Laboratory of Smart Drug Delivery, Ministry of Education, Fudan University, Shanghai 201203, People's Republic of China

*These authors contributed equally to this work

Correspondence: Zheyong Huang; Juying Qian
Department of Cardiology, Zhongshan Hospital, Fudan University, Shanghai Institute of Cardiovascular Diseases, Shanghai 200032, People's Republic of China
Tel +86-21-6404 1990 ext 2153
Fax +86-21-6422 3006
Email zheyonghuang@126.com; qian.juying@zs-hospital.sh.cn

Background: Aortic valve disease is the most common valvular heart disease leading to valve replacement. The efficacy of pharmacological therapy for aortic valve disease is limited by the high mechanical stress at the aortic valves impairing the binding rate. We aimed to identify nanoparticle coating with entire platelet membranes to fully mimic their inherent multiple adhesive mechanisms and target the sclerotic aortic valve of apolipoprotein E-deficient (ApoE$^{-/-}$) mice based on their multiple sites binding capacity under high shear stress.

Methods: Considering the potent interaction of platelet membrane glycoproteins with components present in sclerotic aortic valves, platelet membrane-coated nanoparticles (PNPs) were synthetized and the binding capacity under high shear stress was evaluated in vitro and in vivo.

Results: PNPs demonstrated effectively adhering to von Willebrand factor, collagen and fibrin under shear stresses in vitro. In an aortic valve disease model established in ApoE$^{-/-}$ mice, PNPs exhibited good targeting to sclerotic aortic valves by mimicking platelet multiple adhesive mechanisms.

Conclusion: PNPs could provide a promising platform for the molecular diagnosis and targeting treatment of aortic valve disease.

Keywords: aortic valve, atherosclerosis, platelet membrane, nanoparticle, targeting

Introduction

Aortic valve disease is a progressive disease, primarily presenting with aortic valve sclerosis and leading to aortic valve stenosis later in life.[1] The principal etiology of non-rheumatic aortic stenosis is characterized by inflammatory cell infiltration, increased cellularity, lipid accumulation, extracellular matrix deposition and calcification, which resembles atherosclerosis.[1–4] The narrowing of the aortic orifice ultimately leads to congestive heart failure and sudden cardiac death.[5] However, the only way to treat severe aortic valve stenosis is surgical or transcatheter aortic valve replacement,[6] and no effective therapy has been established for the prevention and early treatment of aortic valve disease. One probable reason for poor effects of drug therapy is the low local drug concentration.[7]

In order to improve local drug concentration, nanoparticles possessing targeting ability have been developed for molecular imaging and targeted therapy in cardiovascular disease,[8,9] which demonstrate many advantages and may provide potential strategy for the development of pharmacological treatment and diagnosis to

aortic stenosis. However, the most important hemodynamic change in aortic stenosis is the increased shear stress, which seriously impairs the binding capacity of nanoparticles due to the increasing dislodging force and detachment rates.[10] Under high shear stress, endothelium was injured and initiated the pathogenesis of aortic stenosis. Then, the subendothelial collagen and von Willebrand factor (vWF) were exposed to blood.[11] Platelets were activated and attached to injured endothelial cells and immobilized vWF on the exposed subendothelium via platelet glycoproteins (GP). Then, slowed platelets engaged collagen and fibrin through adhesive moieties on the platelet surface.[11] Regarding the adhesive functions of platelet, some researchers have decorated nanoparticles with platelet targeting ligands (such as recombinant GP Ibα, GP Ia/IIa and GP VI) to mimic their adhesive function and improve binding function under high shear stress.[10,12] However, mimicking only one adhesive mechanism may not be adequate to efficiently mimic platelet adhesion under physiological flow conditions and a synergistic combination of these adhesions may perform better.[10,13]

In this study, we coated the poly($_{DL}$-lactide-co-glycolic acid) (PLGA) nanoparticles with entire platelet membranes (PNPs) to fully mimic their inherent multiple adhesive mechanisms and target the sclerotic aortic valve of apolipoprotein E-deficient (ApoE$^{-/-}$) mice based on their multiple binding glycoproteins under high shear stress. The binding capacity of PNPs under high shear stress condition was evaluated both in vitro and in a sclerotic aortic valve disease model of ApoE$^{-/-}$ mice fed on cholesterol-rich diet. The enhancement of research into this field is crucial in order to yield potential diagnostic and therapeutic methods and therefore slow the progression of the disease.

Materials and Methods

Materials

Most of the materials were purchased from different biotech companies, described as follows in detail. PLGA (0.67dL/g) (copolymer ratio 50:50) with carboxyl end groups was purchased from LACTEL Absorbable Polymers (USA). Protease inhibitor was purchased from ThermoFisher (USA). Prostaglandin E1 was purchased from MedChem Express (New Jersey, USA). Collagen type IV (human placenta) was purchased from Sigma Aldrich (USA). 1,19-dioctadecyl -3,3,39,39-tetramethylindodicarbocyanine perchlorate (DiD, excitation/emission = 644/665 nm) was purchased from Biotium (USA). Human umbilical vein endothelial cell line (ATCC® PCS-100-010™) was ordered from American Type Culture Collection (USA). Dulbecco's modified Eagle's Medium and fetal serum was purchased from Gibco (Grand Island, USA). Anti-human GPIIb/IIIa antibody was purchased from Biolegend (San Diego, USA). Anti-human GPIb antibody, anti-human Integrin alpha2 antibody, and anti-human Integrin beta1 antibody were purchased from R&D systems (Minnesota, USA). Anti-human GP VI antibody was gained from Merckmillipore (Germany). Polyclonal rabbit anti-fibrinogen/fibrin antibody was purchased from Santa cruz biotechnology (USA). TNF-α was obtained from Prospec (Rehovot, Israel). Sheep polyclonal anti-vWF antibody and polyclonal rabbit anti-collagen IV were gained from abcam (USA). Alexa Fluor 488-labeled donkey anti-rabbit IgG antibody and Alexa Fluor 488-labeled donkey anti-sheep IgG antibody were from Life Technologies (USA). Allophycocyanin-conjugated anti-mouse IgG secondary antibody (GP Ib, beta1), allophycocyanin-conjugated anti-mouse IgM (IIb/IIIa) and allophycocyanin-conjugated anti-rat IgG (GP IV, alpha 2) were purchased from R&D systems (Minnesota, USA). Rabbit anti-CD31 was gained from abcam (USA). Goat anti-rabbit 5-nm gold-conjugated secondary antibody was purchased from Sigma Aldrich (USA).

The following materials were gained from China and detailed below: 1.2-distearoyl-sn-glycero-3-phosphoethanolamine-N-(methoxy(polyethylene glycol)-2000) (DSPE-PEG2000) was purchased from AVT (Shanghai, China). Human type B platelet rich plasma was gained from the Shanghai Blood Bank (Shanghai, China). Fibrinogen and thrombin were obtained from Zhongshan Hospital, Fudan University (Shanghai, China). Male ApoE$^{-/-}$ mice at 8 weeks of age were purchased from the Cavens Biological Technology Co., Ltd. (Jiangsu, China). Von Kossa was purchased from Solarbio life sciences (Beijing, China). The western-type diet with 1.25% cholesterol and 0.5% Sodium cholate was purchased from Changzhou Bo Shan Biological Technology Co., Ltd. (Jiangsu, China).

Methods

Formulation of Nanoparticles

The PLGA nanoparticles were prepared as described previously.[14] Briefly, PLGA was dissolved in acetone, injected into distilled water and then evaporated under vacuum to form PLGA nanoparticles. The nanoparticle solution was then filtered with 10K molecular weight cutoff (MWCO) Amicon Ultra-4 Centrifugal Filters (Millipore) for platelet membrane coating. Platelets were collected

from platelets rich plasma as described previously[14] and platelets membranes were derived by a repeated freeze-thaw process and incubated with 1.2-distearoyl-sn-glycero -3-phosphoethanolamine-N-(methoxy(polyethyleneglycol)-2000) (DSPE-PEG2000) at 37°C for 30 min. Aliquots of platelet solution containing about 3×10^9 platelets were used to cloak 1 mg of PLGA nanoparticles. For PNPs preparation, the PLGA nanoparticles and 1.19-dioctadecyl -3,3,39,39-tetramethylindodicarbocyanine perchlorate (DiD) were mixed with PEGylated platelet membrane and sonicated for 2 min at a power of 100W. As control nanoparticle, DiD labelled PEGylated nanoparticles (NPs) composed of DSPE-PEG2000 and PLGA were synthesized by a nanoprecipitation method as previously described.[14]

Characterization of Nanoparticles

The formulated PLGA cores, PNPs, and NPs were characterized for their morphology, particle size, polydispersity and surface charge (zeta potential) using transmission electron microscopy (H-600, Hitachi, Japan) and dynamic light scattering detector (Malvern Instruments, UK) at room temperature. Immunogold staining analysis was performed to confirm the presentation of platelet membrane marker GP VI on the PNPs.[14] For immunogold TEM, PNPs were pre-incubated with rabbit anti-human GP VI antibodies for 2hrs at room temperature, washed with BSA solution for three times and then incubated with goat anti-rabbit 5-nm gold conjugated secondary antibody for 1hr at room temperature. After washed with BSA solution for three times, the sample was subsequently stained with 2% vanadium solution (Abcam) and visualized using a transmission electron microscopy (H-600, Hitachi, Japan).

Key platelet membrane proteins were also identified by Sodium dodecyl sulfate-polyacrylamide gel electrophoresis (SDS-PAGE) and Western blotting. Briefly, as previously reported,[14,15] platelet membrane vesicles and PNPs were lysed with radio immunoprecipitation assay (RIPA) lysate and the total protein contents in the samples were quantified by a Pierce BCA protein assay kit. Samples mixed with SDS-PAGE sample loading buffer were heated at 100°C for 10 min. Then, samples with equivalent protein amount (40 μg/well) were loaded on 10% SDS-PAGE gel and were run at 120 V for 2 hrs. The resultant gel was stained in Coomassie Blue for 2 hrs and washed overnight for subsequent imaging with GBOX gel documentation system (Bio-Rad, SG). The resulting gel was transferred to polyvinylidene difluoride membranes for Western blot analysis. Membranes were probed with primary antibodies including anti-human GPVI antibody, anti-human GP IIb/IIIa antibody, anti-human GP Ia/IIa antibody, anti-human GP Ibα antibody and anti-human integrin β1 subunit antibody at 4°C overnight, followed by incubation with respective secondary antibody for 1 hr at 37°C. MagicMark XP western protein standard was used as a molecular weight ladder. Then, the membranes were subjected to enhanced chemiluminescence detection kit (BeyoECL Plus, Beyotime, China) and developed with the Mini-PROTEAN Tetra cell (BIO-RAD, SG). Image J (version 1.51) was used to calculate immunoblot signal. Also, membrane glycoproteins of PNPs were identified by flow cytometry, including GPVI, GP IIb/IIIa, GP Ibα, Integrin α2β1.

Mimicking Platelet Adhesive Property in vitro

Coated culture dishes (with vWF, collagen, or fibrin) were assembled in a parallel flow circular chamber (Glycotech, Gaithersburg, MD, USA)[10,12] under varying shear stresses for binding study in vitro. Image J software (version 1.51) was used for calculating the average fluorescence intensity. The PNPs bound intensity at 0 shear rates was arbitrarily set at 100%. To identify the key molecules and mechanisms responsible for PNPs targeting, we also investigated the PNPs binding to vWF, collagen or fibrin on blocking specific biomarkers accordingly.

vWF Binding of PNPs in Flow Chamber Study in vitro

Human umbilical vein endothelial cell was plated onto a glass coverslip, which was the bottom plate of the parallel flow chamber. The plate was maintained in Dulbecco's modified Eagle's Medium containing 10% fetal calf serum and a mixture of glutamine, penicillin, and streptomycin at 37°C in a 5% CO2 humidified incubator. As cells reached 80-90-% confluence, TNF-α recombinant protein (20ng/mL) was added to stimulate human umbilical vein endothelial cells to upregulate vWF expression for 2 hrs.[16] Coverslip with human umbilical vein endothelial cells expressed vWF were placed in the flow chamber. The slides were then exposed to medium containing PNPs (5×10^6/mL) under varying shear stresses (0-25dyn/cm^2) for 30 mins followed by a 5 mins wash using the parallel plate flow chamber system as described previously.[10] And PNPs were incubated with antibodies against GP Ib and GP IIb/IIIa for the antibody blocking experiments.

Collagen Binding of PNPs in Flow Chamber Study in vitro

To examine the effects of shear stress on the binding of PNPs via collagen, microscope slides were coated with 20 μL of the collagen type IV derived from human placenta solution (2.0 mg/mL in 0.25% acetic acid) and incubated overnight at 4°C. The plate was blocked with 2% BSA and washed three times with PBS. Similar to binding study via vWF, PNPs solution (5×10^6/mL) was infused at different shear stresses. PNPs were incubated with antibodies against GP VI and GP Ia/IIa for the antibody blocking experiments.

Fibrin Binding of PNPs in Flow Chamber Study in vitro

Microscope slides, which were coated with 20μL of fibrinogen (2.0mg/mL in PBS), 2μL of 0.4M CaCl2 and 2μL of thrombin (0.1U/mL in PBS), were incubated at 37°C for 60 min and placed in a parallel plate flow chamber. Then, the slides were exposed to medium containing PNPs (5×10^6/mL) solution at different stresses. PNPs were incubated with antibodies against GP IIb/IIIa and GPVI for the antibody blocking experiments.

Animal Protocol of Developing Sclerotic Aortic Valves

The animal experiments were approved by the Animal Care and Use Committee of Zhongshan Hospital and were in compliance with the "Guide for the Care and Use of Laboratory Animals" published by the National Academy Press (NIH Publication No. 85–23, revised 1996). At 8 weeks of age, male $ApoE^{-/-}$ mice were purchased and received a western-type diet (1.25% cholesterol and 0.5% Sodium cholate) for 36 weeks to develop sclerotic aortic valves. Wild-type C57Bl/6J mice were fed regular chow as a control group. After that, mice were anesthetized and Color Doppler imaging was obtained through a parasternal approach with a 30-MHz linear probe and the Vevo 2100 system (VisualSonics, Toronto, Canada). Transaortic valve flow velocity was evaluated by pulse and continuous waves recorded through a near apical approach.[17] After echocardiograms, the aortic valves were harvested and histological examined by Oil Red O staining for valve thickness and lipid deposition, Von Kossa staining for calcification, and immunostaining for an endothelial marker, CD31, for endothelial integrity. The CD31-positive length on the aortic valve surface was calculated as ratio (%) of the total circumference of the aortic valve surface using computer software (MCID 4.0, Imaging Research Inc., St. Catherines, Ontario, Canada) to quantify the integrity of the endothelial cell layer on the aortic valves.[18]

PNPs Adhere and Aggregate on Sclerotic Aortic Valves in $ApoE^{-/-}$ Mice

After 36 weeks of western-type diet, $ApoE^{-/-}$ mice were randomly divided into three groups (n=4) and intravenously injected with 0.5 mg of PNPs, NPs and PBS (100 μL) respectively. Normal C57 mice (n=4) received injection of 0.5 mg of PNPs as control (n=4). Mice were sacrificed at 2 hrs post injection and perfused with 0.9% saline and 4% paraformaldehyde. Aortic valves were harvested, cut into 5-μm cryosections and immunofluorescence stained with antibodies against vWF, collagen or fibrin. The colocalization of PNPs with vWF, collagen or fibrin was investigated under the laser scanning confocal microscopy.

Statistical Analyses

All data are reported as mean ± SE. Comparisons between any two groups were performed using two-tailed unpaired Student's *t*-test. Comparisons among more than two groups were performed using one-way ANOVA followed by posthoc Bonferroni test. Differences were considered statistically significant when $P<0.05$.

Results

Characterization of PNPs

Biomimetic nanoparticle platform to target sclerotic aortic valve was synthesized using the platelet membrane-coated PLGA nanoparticles according to a previously reported method.[14] Theoretically, PNPs binding capacity depends on the platelet glycoproteins, including GP Ib with vWF, GP VI and Integrin α2β1 (GP Ia/IIa) with collagen, GP IIb/IIIa and GP VI with fibrin (Figure 1A). Firstly, transmission electronic microscopy and dynamic light scattering were performed to visualize nanoparticles structure. Transmission electronic microscopy demonstrated the spherical morphology and range size of the NPs and PNPs within 100nm (Figure 1B). Using dynamic light scattering detection, it was determined that PNPs were larger than the bare PLGA cores in size (from 125.4 ± 7.2 nm to 144.3 ± 6.2 nm, $p = 0.026$) (Figure 1C). Compared with NPs, the surface zeta potential of PNPs increased by over 17mV (from −41.8 ± 1.8mV to −24.7 ± 3.5mV, $p = 0.002$) (Figure 1D). Size measurements of PNPs via dynamic light scattering in PBS demonstrated that the size was comparable for 7 days without any significant change in particle size (from 144.3 ± 6.2 nm to 148.2 ± 7.2 nm, $p = 0.52$) (Figure 1E). The mean size and zeta potential of PNPs were

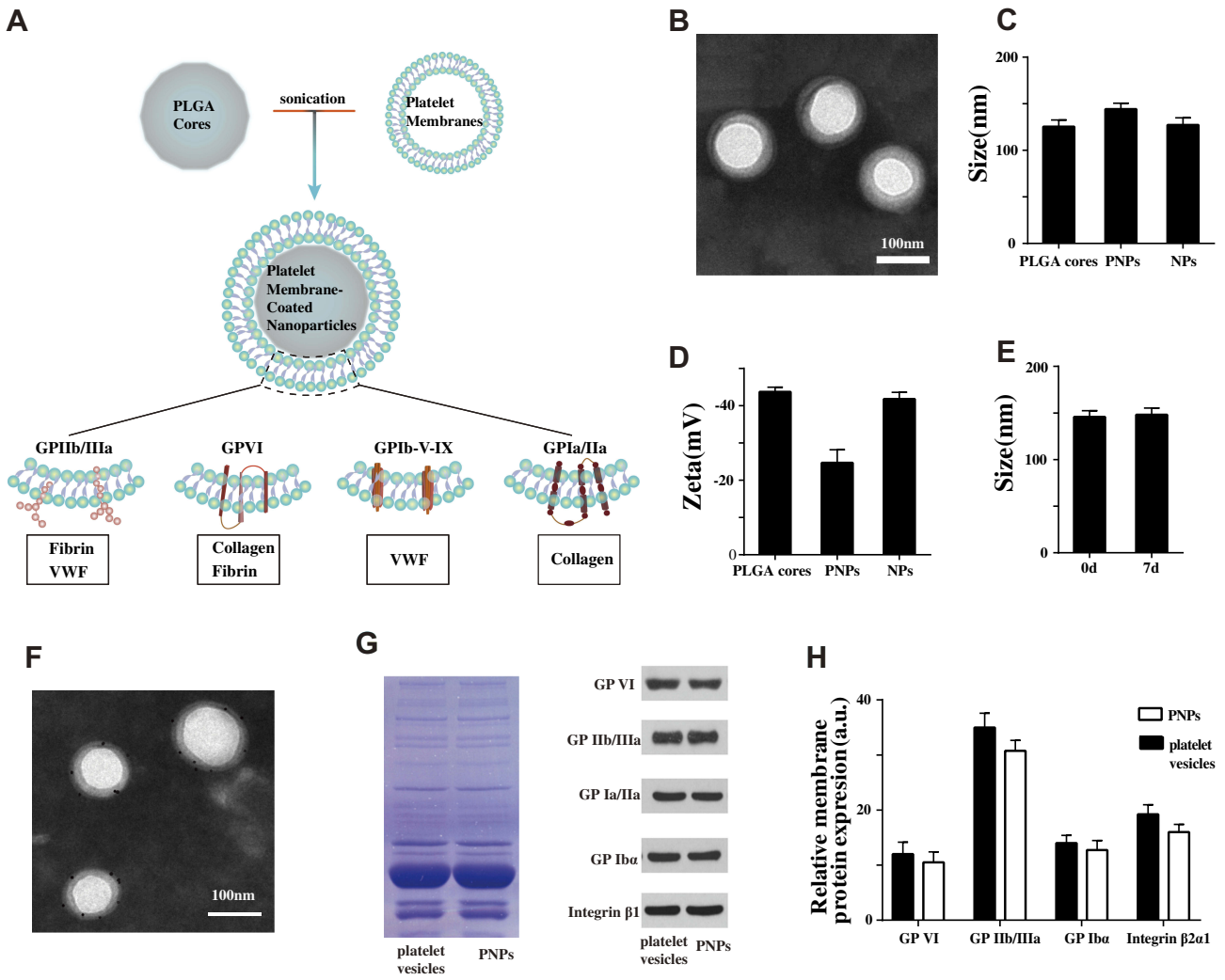

Figure 1 Characterization of PNPs. (**A**) Schematic design of PNPs and the interaction of membrane protein with vWF, Collagen and Fibrin. (**B**) Transmission electron micrographs of PNPs. (**C**) Size of PLGA cores, PNPs and NPs (n=4). (**D**) Zeta potential of PLGA cores, PNPs and NPs (n=4). (**E**) Particle diameter of PNPs in water on day 0 and day 7 (n=4). (**F**) TEM image of PNPs primary stained with anti-GP VI, and secondary stained by an immunogold conjugate. (**G**) Protein content visualization of platelet vesicles and PNPs running on SDS-PAGE at equivalent protein concentrations followed by Coomassie staining and Western blotting analysis of platelet vesicles and PNPs for characteristic platelet membrane markers. All samples were run at equivalent protein concentrations. (**H**) Flow cytometry analysis validated similar platelets glycoproteins. All bars represent means ± s.d.

similar to the results reported in other researchers and our previous study.[14,19] Platelets binding capacity is dependent on their membrane proteins, such as GP Ib to vWF, GP VI and Integrin α2β1 (GP Ia/IIa) to collagen, GP IIb/IIIa and GP VI to fibrin. Immunogold staining analysis was performed to validate the right-side-out membrane orientation on the PNPs. The representative image of immunogold staining with GP VI is displayed in Figure 1F. Translocation of platelet membrane protein content, including GP VI, GP IIb/IIIa, GP Ia/IIa, GP Ibα and Integrin β1, onto the PNPs were examined via Coomassie staining and Western blotting. Western blotting analysis verified that similar membrane protein retention and enrichment were observed between PNPs and platelet vesicles ($p > 0.05$) (Figure 1G). Besides, flow cytometry analysis validated the presence of platelets adhesive antigens such as CP VI, GP IIb/IIIa, GP Ia/IIa, GPIbα and Integrin α2β1 between PNPs and platelet vesicles ($p > 0.05$) (Figure 1H). All the results demonstrated successful membrane coating of PNPs, which remarkably helped to mimic platelets adhesive functions.

Platelet-Mimetic Adhesion of PNPs Under Flow in vitro

Platelet-mimetic adhesions of PNPs to vWF, collagen and fibrin were examined under different flow rates in vitro. The PNPs bound intensity at 0 shear rates was arbitrarily set at 100%. Since PNPs adhesion was accomplished via its

membrane glycoproteins, antibodies were used to confirm the importance of the role of glycoproteins binding to coated surfaces.

PNPs Binding to vWF Under Varying Shear Stresses in vitro

To examine the binding capacity of PNPs to vWF, human umbilical vein endothelial cell line was plated onto a glass coverslip and was stimulated with TNF-α recombinant protein to upregulate vWF expression. Figure 2 shows that PNPs bound intensity to vWF was increased as the shear stress increased until the shear stress reached 20 dyn/cm^2, while NPs poorly bound to vWF irrespective of shear stress values. And under shear stress condition of 25dyn/cm^2, PNPs bound intensity was about 1.61-fold of that at static state. The normalized intensity of PNPs binding with vWF was 119%, 133%, 145%, 204% and 161% under different shear stress of 5, 10, 15, 20 and 25dyn/cm^2, and the normalized intensity of NPs was 12.0%, 7.9%, 5.9%, 4.8%, 4.0% and 4.0% under different shear stress of 0, 5, 10, 15, 20 and 25dyn/cm^2, respectively) (p<0.001 at different shear stress). Since the binding of platelets to vWF was mediated by GP Ib and GP IIb/IIIa, PNPs were incubated with antibodies against GP Ib and GP IIb/IIIa for the antibody blocking experiments. Statistical analysis of fluorescence intensity values showed minimal adhesion of PNPs with blocking antibodies, indicating the essential role of GP Ib and GP IIb/IIIa in the PNPs targeting abilities to vWF.

PNPs Binding to Collagen Under Varying Shear Stresses in vitro

Figure 3 shows the representative set of fluorescence images of PNPs on collagen-coated surfaces under flow. Quantitative analysis showed PNPs undergone significant adhesion to collagen under flow with no apparent shear-dependent effect. Compared with PNPs bound intensity in the static station, 94.2%, 90.0%, 78.0%, 72.0% and 59.0% of the attached PNPs remained adherent on collagen-coated surfaces under different shear stress of 5, 10, 15, 20 and 25dyn/cm^2. In the control group, 14.2%, 11.7%, 8.4%, 7.1%, 5.1% and 4.5% of unmodified nanoparticles remained adherent on collagen-coated surfaces under different shear stress of 0, 5, 10, 15, 20 and 25dyn/cm^2 respectively (p<0.001 at different shear stress). Also, the blocking experiments were produced with antibodies of GP VI and GP Ia/IIa. With antibodies against GP VI and GP Ia/IIa, PNPs bound density to collagen-coated surfaces was significantly reduced, which indicated that platelet membrane proteins, GP VI and GP Ia/IIa, played an important role in PNPs binding to collagen.

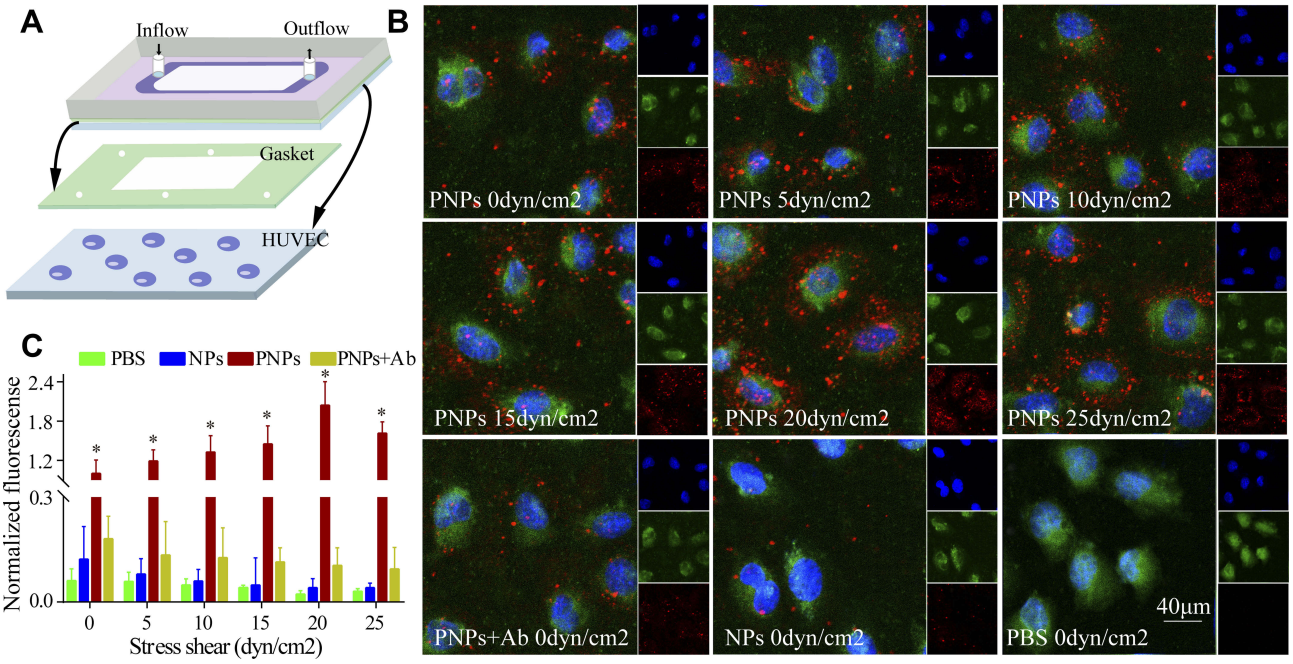

Figure 2 Mimicking the platelets adhesive function of PNPs via vWF in vitro. (**A**) Schematic design of parallel flow circular chamber study of vWF. (**B**) Representative fluorescent microscopic images showing the binding of PNPs (red) to vWF (green) under varying shear stresses, and PBS, NPs and PNPs incubating with antibodies (PNPs + Ab) at 0 shear rates. (**C**) Normalized nanoparticle bound intensity under different shear rates. The PNPs bound intensity at 0 shear rates was arbitrarily set at 100%. *p<0.001 compared with any other group under the same stress shear. All bars represent means ± s.d.

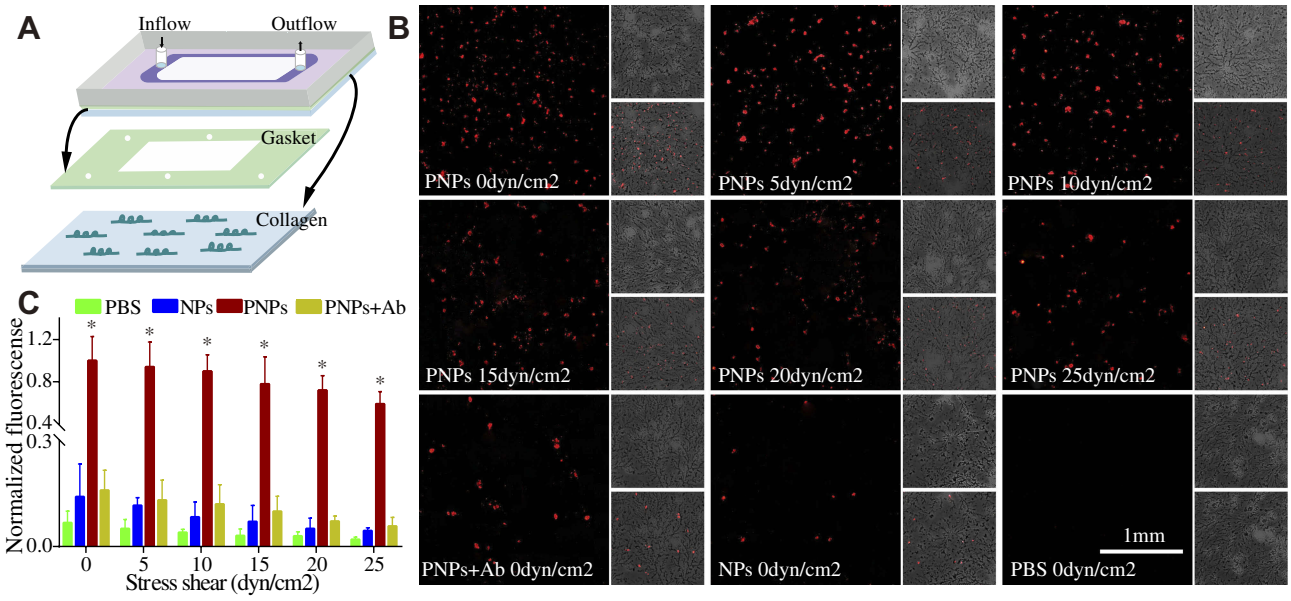

Figure 3 Mimicking the platelets adhesive function of PNPs via collagen in vitro. (**A**) Schematic design of parallel flow circular chamber study of collagen. (**B**) Representative fluorescent microscopic images showing the binding of PNPs (red) to collagen (green) under varying shear stresses, and PBS, NPs and PNPs incubating with antibodies (PNPs + Ab) at 0 shear rates. (**C**) Normalized nanoparticle bound intensity under different shear rates. The PNPs bound intensity at 0 shear rates was arbitrarily set at 100%. *p<0.001 compared with any other group under the same stress shear. All bars represent means ± s.d.

PNPs Binding to Fibrin Under Varying Shear Stresses in vitro

Similar to the results of PNPs binding to collagen, PNPs showed significantly adhesion on the fibrin-coated surface under flow and NPs showed minimal adhesion on fibrin surfaces. And as evident from the fluorescent images as well as the quantitative data, the intensity of adhered PNPs were significantly higher than unmodified NPs at all shear stresses. Compared with PNPs bound intensity in the static station, 95.0%, 96.0%, 69.0%, 55.0% and 39.0% of attached PNPs remained adherent on fibrin-coated surfaces under different shear stress of 5, 10, 15, 20 and 25dyn/cm^2. In the control group, 11.4%, 10.9%, 6.8%, 5.8%, 4.3% and 3.1% of unmodified nanoparticles remained adherent on fibrin-coated surfaces under different shear stress of 0, 5, 10, 15, 20 and 25dyn/cm^2 respectively (p<0.001 at different shear stress). In addition, PNPs incubated with antibodies of GP IIb/IIIa and GP VI significantly reduced fibrin binding, indicating the important role of GP IIb/IIIa and GP VI in the PNPs binding to fibrin (Figure 4).

Targeting to Sclerotic Aortic Valves of PNPs in ApoE$^{-/-}$ Mice

ApoE$^{-/-}$ mice fed on high-fat diet could develop sclerotic aortic valves that resembled human aortic stenosis.[2] In this study, ApoE$^{-/-}$ mice were fed with high cholesterol diet for 36 weeks to develop sclerotic aortic valves. The echocardiography showed that ApoE$^{-/-}$ mice group displayed increased transaortic valve flow velocity compared with control group (Figure 5A–C, ApoE$^{-/-}$ mice 750 ± 57.2 mm/s VS control group 417 ± 15.3 mm/s, $p < 0.001$). Next, the sclerotic aortic valves were examined histologically. Increased valve thickness, oil red stained, calcification and destroyed endothelial integrity were observed in the ApoE$^{-/-}$ mice and are shown in Figure 5D. Quantitative analysis revealed significantly thicker valves in ApoE$^{-/-}$ mice than in wild-type C57 mice (110.8 ± 26.2 mm vs 37.9 ± 9.3 mm, $p < 0.001$) (Figure 5D). Von Kossa staining revealed ectopic calcification in the aortic valves of ApoE$^{-/-}$ mice, while little calcification was detected in the aortic valves of C57 mice (1.58 ± 0.23% vs 0.52 ± 0.13%, $p <$ 0.001). Meanwhile, the endothelial integrity of the aortic valve was disrupted in ApoE$^{-/-}$ mice, while valve leaflets of C57 mice were covered with an endothelial cell layer by detection of CD31-immunofluorescence positive length on the valve surface (42.3 ± 8.3% vs 69.9 ± 9.0%, p <0.001) (Figure 5D). ApoE$^{-/-}$ mice were intravenously injected with respective nanoparticles to evaluate the targeting ability of PNPs to sclerotic aortic valves in vivo. After 2 hrs of administration, the aortic roots were harvested, embedded and cut for further analyzed. As showed in Figure 6, PNPs group exhibited significant increase of accumulation in the aortic valves compared with PBS and control NP group. To

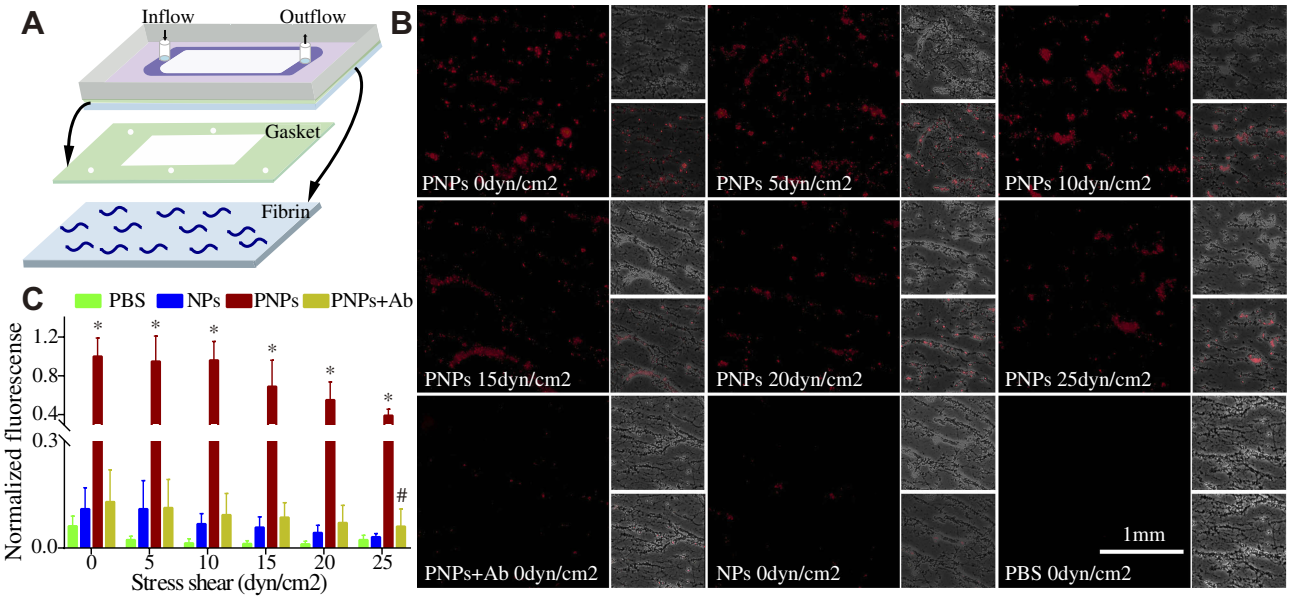

Figure 4 Mimicking the platelets adhesive function of PNPs via fibrin in vitro. (**A**) Schematic design of parallel flow circular chamber study of fibrin. (**B**) Representative fluorescent microscopic images showing the binding of PNPs (red) to fibrin (green) under varying shear stresses, and PBS, NPs and PNPs incubating with antibodies (PNPs + Ab) at 0 shear rates. (**C**) Normalized nanoparticle bound intensity under different shear rates. The PNPs bound intensity at 0 shear rates was arbitrarily set at 100%. *p<0.001 compared with any other group under the same stress shear. All bars represent means ± s.d. #p<0.01 compared with PBS group.

verify the binding effect was specific to sclerotic aortic valves, C57 mice with healthy aortic valves were used to repeat the experiments and PNPs showed minimal binding to healthy aortic valves. To obtain more details about the binding, the sections were then stained with separate antibodies to probe for various elements of sclerotic aortic valves, such as antibodies for vWF, collagen and fibrin. As showed in Figure 6, PNPs displayed high degrees of proximity or co-localization with vWF, collagen and fibrin. The results suggest that PNPs with natural platelet membrane coated could effectively and specifically target to sclerotic aortic valves with multiple sites binding.

Discussion

In this study, we described the usage of PNPs for targeting sclerotic aortic valves by their fully mimicked platelets adhesive functions with multiple biological elements under high shear stress.

Platelets adhesion is mediated by shear-dependent binding with vWF secreted from the injured endothelium, and augmented by binding to subendothelial collagen. These adhesive mechanisms result in platelet activation signaling, ultimately leading to a ligand-binding conformational change of the platelet surface integrin GP IIb/IIIa, which then binds to fibrin to promote aggregation of the activated platelets to form the primary hemostatic plug.[11] Design of platelet-inspired synthetic adhesive functions should aim to adapting various functional components of these natural phenomena, especially at pathological shear stress. In healthy individuals, shear stress at 15dyn/cm^2 and flow velocity at 1.4m/s are presented as the average arterial flow condition.[20–22] Mice aortic flow velocities are less than human values.[17] As the stenosis progresses, blood velocity and shear stress across the aortic valve dramatically increase both in mice and human.[1,23,24] In previous studies, microbubbles were modified with antibodies against E- and P-selectin to enhance targeting ability. Though the microbubbles exhibited well adhesion at low shear stress, they undergone significantly decreased binding as the shear stress increased.[25,26] And nanoparticles modified with GPIb, which played an essential role in platelet adhesion under high shear flow conditions, also revealed decreased binding under shear stress of 25dyn/cm^2.[10] These results illustrated that the bottom-up approaches which decorated the particle surface with targeting ligands of platelets were difficult to truly mimic the platelets binding function under the shear stress and effectively target the regions of interest.

Currently, the top-down approaches, which the nanoparticles were cloaked with entire platelet membranes to represent the biological complexity on the carrier's surface and maintain their natural targeting ability, have caught

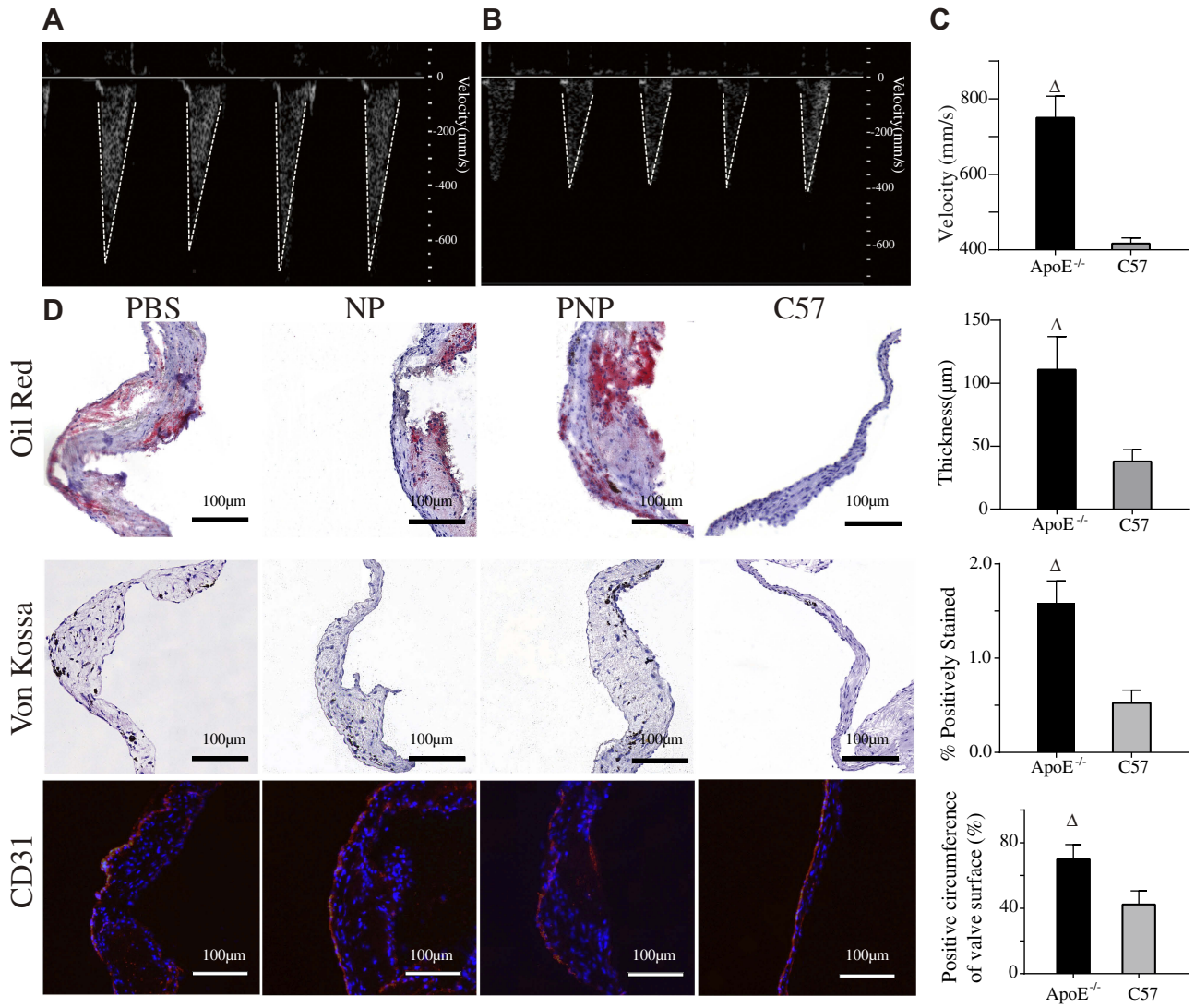

Figure 5 Proof of sclerosis. Representative Doppler images of ApoE$^{-/-}$ mice (**A**), C57 mice (**B**) and quantitative results of transaortic valve flow velocity (**C**). Δ $p<0.001$. (**D**) Representative aortic valve sections and quantitative results of thickness, calcification, and destroyed endothelial integrity. $^{\Delta}p<0.01$.

increasing attention. And the recent studies have demonstrated the application of platelets' membrane-coated nanoparticles in several diseases, such as artery diseases,[9,14,27] bacterial infection,[14] immune thrombocytopenia,[28] and cancer.[29,30] In this study, we evaluated the mimicry of platelets multiple adhesive mechanisms of PNPs at different shear stresses.

PNPs possessed increased binding to vWF with increasing shear in vitro study, and the intensity of PNPs bound to vWF at shear stress of 25dyn/cm^2 was 1.61-fold that in the static station. After incubated with antibodies against GP Ib and GP IIb/IIIa, PNPs significantly reduced vWF binding. Platelet membrane decorating significantly enhanced the shear-dependent adhesion of PNPs by the specific interaction between platelet membrane proteins and vWF. Compared with unmodified nanoparticles, PNPs also showed significant adhesion to collagen and fibrin-coated surfaces under over the entire shear stress. Under low shear stress, up to 10dyn/cm^2, the intensity of PNPs bound to collagen and fibrin was not significantly changed. Respectively, 59% and 39% of attached PNPs remained adherent on collagen- and fibrin-coated surfaces under high shear stress of 25dyn/cm^2, revealing that the adhesion of PNPs to collagen and fibrin was more efficient in lower shear stress environments. In vitro studies showed that PNPs possessed efficient adhesion to collagen and fibrin in lower shear stress[11,31] and to vWF in higher shear stress,[11,32,33] which mimicked the platelets multiple adhesive mechanisms under physiologically relevant flow conditions by platelets membrane coating.

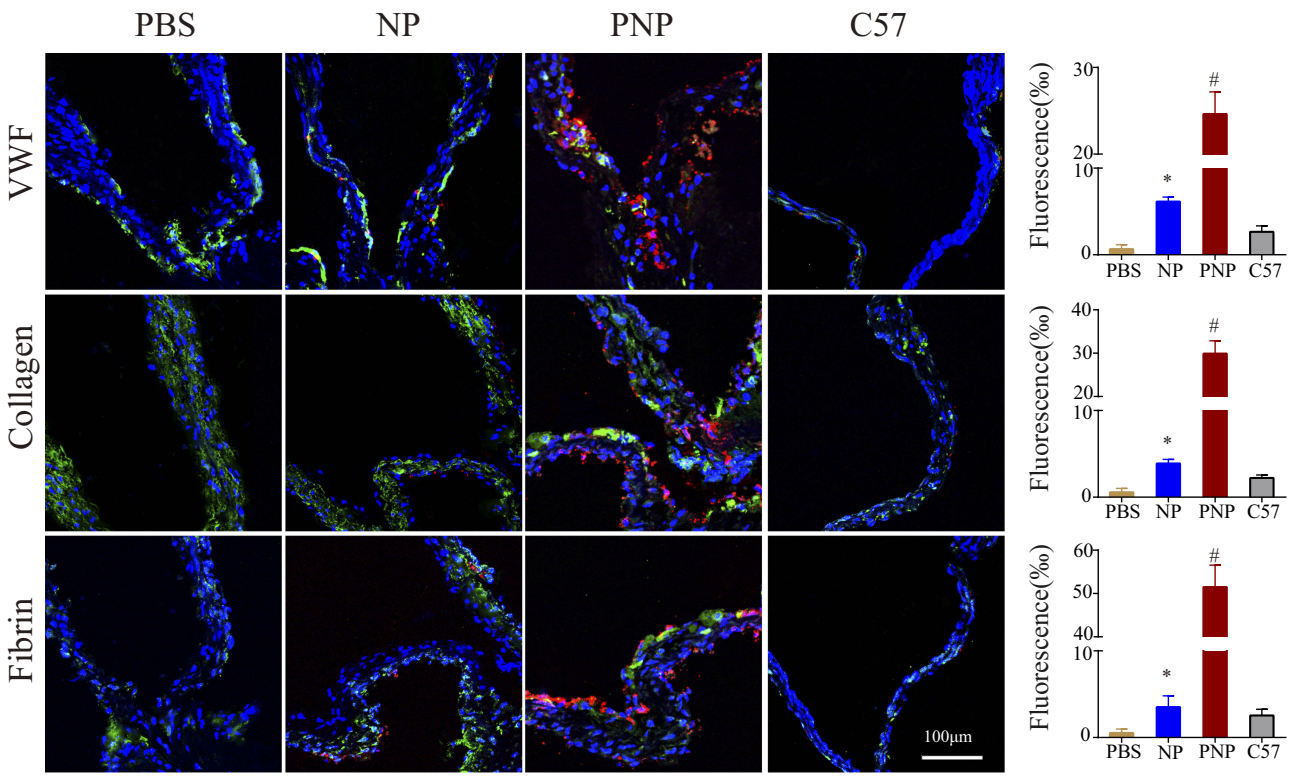

Figure 6 PNPs accumulation in sclerotic aortic valves of ApoE$^{-/-}$ mice in vivo. The representative fluorescent microscopic images and quantitative results of fluorescence which confirmed the enhanced PNPs (red) targeting to sclerotic aortic valves and co-localization with vWF, collagen and fibrin in ApoE$^{-/-}$ mice. *p<0.01 compared with PBS group, $^{\#}p$<0.01 compared with any other group. All bars represent means ± s.d.

In degenerative aortic stenosis, significant pathological changes occurred in the aortic side. Collagen is the major protein of the total protein of the valve.[33] The expression of vWF and fibrin deposition are significantly increased in the aortic stenotic valves.[34,35] The overexpressed antigens might be helpful for PNPs targeting diseased aortic valves. In vivo study showed that PNPs could effectively adhere to sclerotic aortic valves under pathological shear stress and co-localized with vWF, collagen and fibrin, which indicated that the remarkable binding ability of PNPs was mainly due to the multiple sites combinations between the full adhesive molecules of platelet membranes coating on PNPs and the overexpressed antigens of sclerotic aortic valves, including vWF, collagen and fibrin.

In this study, ApoE$^{-/-}$ mice fed a cholesterol diet had significantly thicker aortic valve leaflets and increased aortic flow velocity. The average aortic flow velocity was about 750mm/s, which represented the mild aortic valve stenosis.[2] Presently, the treatment of aortic valve stenosis relies on the replacement of the aortic valve in patients with severe, symptomatic aortic stenosis and no effective pharmacological therapy has been estimated to reduce the progression rate of aortic stenosis. From a clinical standpoint, a pharmacotherapy could be started in patients with mild and/or moderate aortic stenosis, our study has certain clinical significance for the molecular diagnosis and treatment of aortic stenosis in the early stage. And the targeting efficiency of PNPs should be further studied in severe aortic stenosis in vivo.

Though PNPs are attracting increasing attention and have shown great promise for clinical applications, it is still in infancy stage. Multiple challenges need to be overcome before clinical application, such as the shortage of platelets, immunogenicity, and heterogeneity in clinic use. The shortage of platelet prompts technology improvement using less platelet membrane and maintaining the targeting ability. Autologous or blood type matching platelets may be helpful to avoid immunoreactions and the major adhesive glycoproteins should be tested to ensure the effect. With the development of technology, reliable PNPs production would be envisioned for clinical translation.

In summary, PNPs successfully mimicked the platelets multiple binding mechanisms at different shear stresses and targeted effectively to sclerotic aortic valves in ApoE$^{-/-}$ mice based on the inherent interaction of platelet membrane binding moieties with multiple components present in sclerotic aortic valves, including vWF, collagen and fibrin.

Conclusion

As a novel targeting platform, platelet membrane-coated nanoparticles were synthetized and demonstrated effective adhesion under high shear stresses both in vitro and in vivo. By encapsulating imaging molecule or drugs, PNPs may provide a promising platform for the molecular diagnosis and target treatment of mild and/or moderate aortic stenosis, thus improving the prognosis of patients with aortic valve disease.

Acknowledgments

This study was financially supported by the National Natural Science Foundation of China (grants 81801374, 81870269, 81600199, 81773283 and 81570223).

Disclosure

The authors report no conflicts of interest in this work.

References

1. Baumgartner H, Falk V, Bax JJ, et al. 2017 ESC/EACTS guidelines for the management of valvular heart disease. *Eur Heart J*. 2018;38:2739–2791. doi:10.1093/eurheartj/ehx391
2. Aikawa E, Nahrendorf M, Sosnovik D, et al. Multimodality molecular imaging identifies proteolytic and osteogenic activities in early aortic valve disease. *Circulation*. 2007;115(3):377–386. doi:10.1161/CIRCULATIONAHA.106.654913
3. Drolet MC, Roussel E, Deshaies Y, et al. A high fat/high carbohydrate diet induces aortic valve disease in C57BL/6J mice. *J Am Coll Cardiol*. 2006;47(4):850–855. doi:10.1016/j.jacc.2005.09.049
4. Miller JD, Weiss RM, Serrano KM, et al. Lowering plasma cholesterol levels halts progression of aortic valve disease in mice. *Circulation*. 2009;119(20):2693–2701. doi:10.1161/CIRCULATIONAHA.108.834614
5. Otto CM, Prendergast B. Aortic-valve stenosis–from patients at risk to severe valve obstruction. *N Engl J Med*. 2014;371:744–756. doi:10.1056/NEJMra1313875
6. Slomski A. TAVR vs surgery in low-risk patients. *JAMA*. 2019;321:1965.
7. Cowell SJ, Newby DE, Prescott RJ, et al. A randomized trial of intensive lipid-lowering therapy in calcific aortic stenosis. *N Engl J Med*. 2005;352:2389–2397. doi:10.1056/NEJMoa043876
8. Jain AK, Das M, Swarnakar NK, et al. Engineered PLGA nanoparticles: an emerging delivery tool in cancer therapeutics. *Crit Rev Ther Drug Carrier Syst*. 2011;28:1–45. doi:10.1615/CritRevTherDrugCarrierSyst.v28.i1.10
9. Wei X, Ying M, Dehaini D, et al. Nanoparticle functionalization with platelet membrane enables multifactored biological targeting and detection of atherosclerosis. *ACS Nano*. 2018;12:109–116. doi:10.1021/acsnano.7b07720
10. Kona S, Dong JF, Liu Y, et al. Biodegradable nanoparticles mimicking platelet binding as a targeted and controlled drug delivery system. *Int J Pharm*. 2012;423:516–524. doi:10.1016/j.ijpharm.2011.11.043
11. Chen J, Lopez JA. Interactions of platelets with subendothelium and endothelium. *Microcirculation*. 2005;12:235–246. doi:10.1080/10739680590925484
12. Ravikumar M, Modery CL, Wong TL, et al. Mimicking adhesive functionalities of blood platelets using ligand-decorated liposomes. *Bioconjug Chem*. 2012;23:1266–1275. doi:10.1021/bc300086d
13. Modery-Pawlowski CL, Tian LL, Pan V, et al. Approaches to synthetic platelet analogs. *Biomaterials*. 2013;34:526–541. doi:10.1016/j.biomaterials.2012.09.074
14. Hu CM, Fang RH, Wang KC, et al. Nanoparticle biointerfacing by platelet membrane cloaking. *Nature*. 2015;526:118–121. doi:10.1038/nature15373
15. Jiang Q, Liu Y, Guo R, et al. Erythrocyte-cancer hybrid membrane-camouflaged melanin nanoparticles for enhancing photothermal therapy efficacy in tumors. *Biomaterials*. 2019;192:292–308. doi:10.1016/j.biomaterials.2018.11.021
16. Guo S, Shen S, Wang J, et al. Detection of high-risk atherosclerotic plaques with ultrasound molecular imaging of glycoprotein IIb/IIIa receptor on activated platelets. *Theranostics*. 2015;5:418–430. doi:10.7150/thno.10020
17. Pollick C, Hale SL, Kloner RA. Echocardiographic and cardiac Doppler assessment of mice. *J Am Soc Echocardiogr*. 1995;8:602–610. doi:10.1016/S0894-7317(05)80373-6
18. Arishiro K, Hoshiga M, Negoro N, et al. Angiotensin receptor-1 blocker inhibits atherosclerotic changes and endothelial disruption of the aortic valve in hypercholesterolemic rabbits. *J Am Coll Cardiol*. 2007;49:1482–1489. doi:10.1016/j.jacc.2006.11.043
19. Song Y, Huang Z, Liu X, et al. Platelet membrane-coated nanoparticle-mediated targeting delivery of Rapamycin blocks atherosclerotic plaque development and stabilizes plaque in apolipoprotein E-deficient (ApoE(−/−)) mice. *Nanomedicine*. 2019;15:13–24. doi:10.1016/j.nano.2018.08.002
20. Gould ST, Srigunapalan S, Simmons CA, et al. Hemodynamic and cellular response feedback in calcific aortic valve disease. *Circ Res*. 2013;113:186–197. doi:10.1161/CIRCRESAHA.112.300154
21. Yap CH, Saikrishnan N, Yoganathan AP. Experimental measurement of dynamic fluid shear stress on the ventricular surface of the aortic valve leaflet. *Biomech Model Mechanobiol*. 2012;11:231–244. doi:10.1007/s10237-011-0306-2
22. Sun L, Rajamannan NM, Sucosky P. Design and validation of a novel bioreactor to subject aortic valve leaflets to side-specific shear stress. *Ann Biomed Eng*. 2011;39:2174–2185. doi:10.1007/s10439-011-0305-6
23. Tanaka K, Sata M, Fukuda D, et al. Age-associated aortic stenosis in apolipoprotein E-deficient mice. *J Am Coll Cardiol*. 2005;46:134–141. doi:10.1016/j.jacc.2005.03.058
24. Wang W, Vootukuri S, Meyer A, et al. Association between shear stress and platelet-derived transforming growth factor-beta1 release and activation in animal models of aortic valve stenosis. *Arterioscler Thromb Vasc Biol*. 2014;34:1924–1932. doi:10.1161/ATVBAHA.114.303852
25. Dickerson JB, Blackwell JE, Ou JJ, et al. Limited adhesion of biodegradable microspheres to E- and P-selectin under flow. *Biotechnol Bioeng*. 2001;73:500–509. doi:10.1002/bit.1085
26. Takalkar AM, Klibanov AL, Rychak JJ, et al. Binding and detachment dynamics of microbubbles targeted to P-selectin under controlled shear flow. *J Control Release*. 2004;96:473–482. doi:10.1016/j.jconrel.2004.03.002
27. Dehaini D, Wei X, Fang RH, et al. Erythrocyte-platelet hybrid membrane coating for enhanced nanoparticle functionalization. *Adv Mater*. 2017;29(16). doi:10.1002/adma.201700681
28. Wei X, Gao J, Fang RH, et al. Nanoparticles camouflaged in platelet membrane coating as an antibody decoy for the treatment of immune thrombocytopenia. *Biomaterials*. 2016;111:116–123. doi:10.1016/j.biomaterials.2016.10.003
29. Hu Q, Sun W, Qian C, et al. Anticancer Platelet-Mimicking Nanovehicles. *Adv Mater*. 2015;27:7043–7050. doi:10.1002/adma.201503323
30. Wang C, Sun W, Ye Y, et al. In situ activation of platelets with checkpoint inhibitors for post-surgical cancer immunotherapy. *Nat Biomed Eng*. 2017;1(2). doi:10.1038/s41551-016-0011
31. Savage B, Saldivar E, Ruggeri ZM. Initiation of platelet adhesion by arrest onto fibrinogen or translocation on von Willebrand factor. *Cell*. 1996;84:289–297. doi:10.1016/S0092-8674(00)80983-6

32. Nishiya T, Murata M, Handa M, et al. Targeting of liposomes carrying recombinant fragments of platelet membrane glycoprotein Ibalpha to immobilized von Willebrand factor under flow conditions. *Biochem Biophys Res Commun*. 2000;270:755–760. doi:10.1006/bbrc.2000.2516
33. Bashey RI, Torii S, Angrist A. Age-related collagen and elastin content of human heart valves. *J Gerontol*. 1967;22:203–208. doi:10.1093/geronj/22.2.203
34. Natorska J, Marek G, Hlawaty M, et al. Fibrin presence within aortic valves in patients with aortic stenosis: association with in vivo thrombin generation and fibrin clot properties. *Thromb Haemost*. 2011;105:254–260. doi:10.1160/TH10-09-0612
35. Hakuno D, Kimura N, Yoshioka M, et al. Periostin advances atherosclerotic and rheumatic cardiac valve degeneration by inducing angiogenesis and MMP production in humans and rodents. *J Clin Invest*. 2010;120:2292–2306. doi:10.1172/JCI40973